Eur. Phys. J. D **36**, 173–178 (2005)
DOI: 10.1140/epjd/e2005-00223-5

THE EUROPEAN PHYSICAL JOURNAL D

Radiative relaxation in 2p-excited argon clusters

Evidence for the interatomic Coulombic decay mechanism

I.L. Bradeanu[1], R. Flesch[1], M. Meyer[2], H.-W. Jochims[3], and E. Rühl[1,a]

[1] Institut für Physikalische Chemie, Universität Würzburg, Am Hubland, 97074 Würzburg, Germany
[2] LURE, Centre Universitaire Paris-Sud, Bâtiment 209D, 91898 Orsay Cedex, France
[3] Physikalische Chemie, Freie Universität Berlin, Takustr. 3, 14195 Berlin, Germany

Received 15 April 2005 / Received in final form 7 June 2005
Published online 9 August 2005 –

Abstract. The emission of ultraviolet fluorescence radiation from variable size argon clusters is investigated with high spectral resolution in the Ar 2*p*-excitation regime. The fluorescence excitation spectra reveal strong fluorescence intensity in the Ar 2*p*-continuum, but no evidence for the occurrence of discrete low-lying core-exciton states in the near-edge regime. This finding is different from the absorption and photoionization cross section of argon clusters and the solid. The dispersed fluorescence shows a broad molecular band centered near 280 nm. The present work indicates that double and triple ionization via the LMM-Auger decay are required to initiate the fluorescence processes in the Ar 2*p*-continuum. The present results are consistent with the formation of singly charged, excited moieties within the clusters, which are assigned as sources of the radiative emission in the 280 nm regime. A fast energy transfer process (interatomic Coulombic decay (ICD)), which has been proposed by recent theoretical work, is assigned to be primarily the origin of these singly charged, excited cations besides intra-cluster electron impact ionization by the Auger electrons. Our findings give first possible experimental evidence for ICD in the core level regime.

PACS. 32.30.Rj X-ray spectra – 36.40.Mr Spectroscopy and geometrical structure of clusters

1 Introduction

Relaxation processes occurring in the regime of inner-shell excitation and inner-valence shell excitation have been subject of several recent studies. Cederbaum and coworkers have predicted from theoretical work that there is a fast energy transfer process which is active in the inner-valence shell [1–5] as well as in the core level regime [6]. This process is called interatomic Coulombic decay (ICD), which is found to be dominant compared to other possible relaxation processes, such as charge transfer. In the inner-valence shell regime such fast energy transfer processes are expected to occur in dimers and clusters below the threshold of direct double ionization of the corresponding isolated species. More recently, first experimental evidence for the occurrence of ICD in the inner-valence shell regime has been reported [7–9].

The emission of ultraviolet and vacuum ultraviolet radiation from gaseous and solid argon has been the subject of numerous studies in the past, where several continua are observed [10–24]. Specifically, the assignment of the molecular continua has been the subject of debate, where the "first" and the "second continuum" emission are quite well understood. However, the mechanisms leading to the emission of the "third continuum" are not fully known, even though several attempts for its interpretation have been made. There are two different plausible assignments: (i) the radiative decay of singly charged, excited argon molecules gives rise to the emission of "third continuum" radiation [13,20,22] and (ii) doubly charged atomic cations are considered, which decay after having formed charge transfer excimers into two singly charged cations [14,15]. Moreover, the potential energy curves of excited molecular states have been calculated in order to elucidate the origin of the emission process [23,24]. It has been pointed out in more recent work that there is not only one "third continuum" rather than several continua, which reflect different radiative processes and may explain the experimental findings in earlier spectroscopic work [17]. This is consistent with a more recent study by Wieser et al. [19], where systematic time resolved experiments using particle beam excitations were performed.

We have investigated earlier the "third continuum" of 2*p*-excited argon clusters by dispersed fluorescence spectroscopy [25]. However, there were several drawbacks and uncertainties with this experimental work. Specifically, the energy resolution ($E/\Delta E \approx 150$) of the soft X-ray monochromator used for the Ar 2*p*-excitation was quite

[a] e-mail: eruehl@phys-chemie.uni-wuerzburg.de

poor (cf. Ref. [26]) and did not allow us to resolve properly the core-excited Rydberg- and exciton-states. Moreover, the resolution of the secondary vacuum monochromator was also fairly low ($\Delta\lambda \approx 5$ nm), so that is was not clear whether narrow features would occur, if a high-resolution set-up is used. This is the main motivation for the present work, where we have overcome these experimental drawbacks. We re-examine the emission of ultraviolet radiation initiated by Ar $2p$-excitation of variable size argon clusters. Besides the experimental progress, our work is also stimulated by recent theoretical and experimental studies on fast relaxation pathways after primary inner-valence shell- and core-level-excitation of van der Waals dimers and clusters [1–9]. Together with these results, the present work provides new insight into the relaxation processes occurring in $2p$-excited argon clusters. This allows us to derive a plausible mechanism on the radiative processes of core-excited rare gas clusters, which can also be applied to the corresponding solids.

2 Experimental

The experimental set-up consists of a continuous supersonic jet that is used for variable size argon cluster preparation. The stagnation temperature in the high-pressure reservoir of the jet expansion containing the argon (commercial sample (Messer Griesheim), purity: 99.99%) is varied at a stagnation pressure of 5 bar between −120 °C and room temperature. This corresponds to average cluster sizes $\langle N \rangle$ ranging between 200 and 10 using the size calibration procedure of Karnbach et al. [27]. Note that the average cluster size is estimated to be between 750 and 50, if the calibration of Farges et al. [28] is used. The cluster jet is excited by monochromatic synchrotron radiation at the U49/2-PGM1-beam line of the electron storage ring BESSY-II (Berlin, Germany). The first harmonic of the undulator is used and the monochromator is operated with a 600 ℓ/mm plane grating. The energy resolving power ($E/\Delta E$) of the beam line is higher than 5×10^3, as evidenced from photoion yield and fluorescence excitation spectra of the atom in the Ar $2p$ regime (cf. Fig. 1). The total fluorescence in the ultraviolet regime is detected by a cooled photomultiplier tube, which is mounted behind a quartz window (EMI 9789QB), similar to previous work [25]. This set-up is also used to measure fluorescence excitation spectra. The dispersed fluorescence is collected in the ultraviolet/visible regime by a spherical mirror and a UV silica lens. It is focused onto the entrance slit of a secondary Czerny-Turner monochromator with a focal length of 460 mm (HRS-460, Jobin-Yvon, $f/5.3$). This device is equipped with a 300 ℓ/mm grating providing an ultimate wavelength resolution of 0.2 nm [29,30]. The resolution is set during the experiments to 1.5 nm, as established from the atomic argon transitions. The fluorescence light is detected by a liquid nitrogen cooled CCD-detector with a chip size of 800 × 2000 pixels (Lumogen&VISAR, SITe (Tektronix)). The spectral detection covers the range from 200 nm to 1000 nm with a quantum efficiency of the order of 25% in the ultraviolet regime. The transmission function of the spectrograph is estimated to be low at wavelengths below 250 nm. It reaches ∼10% at 300 nm and increases to ∼50% at 500 nm [29,30]. The energy scale of the spectrograph is calibrated using the known fluorescence transitions of atomic argon [31,32] and the molecular nitrogen cation (B-X-transitions) [33,34], respectively. This allows us to calibrate the absolute wavelength scale with an accuracy of smaller than 1 nm. The dispersed fluorescence signal is weak. Therefore, the signal strength is substantially increased by tuning the undulator gap to the appropriate photon energy (245−265 eV), while leaving the X-ray monochromator in zeroth order. The harmonic of the undulator radiation is found to have a slightly asymmetric profile as a function of the photon energy with a typical band width of photon energy in the Ar $2p$ excitation regime of 6 eV for the full width half maximum. This is sufficient for experiments in the Ar $2p$-continuum of variable size clusters, where only broad continuum features are observed [35,36]. Total and partial cation yields are measured using a time-of-flight mass spectrometer, which has been described before in greater detail [36,37].

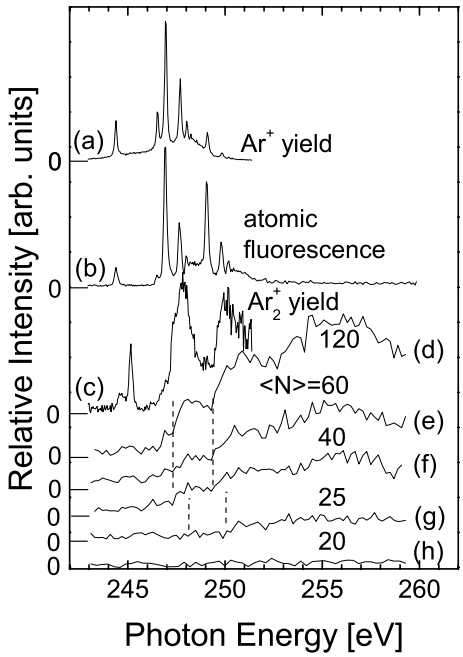

Fig. 1. Comparison of the Ar^+ yield, the total fluorescence excitation spectrum of atomic argon [(a) and (b)] and the Ar_2^+ yield [(c)] with a series of fluorescence excitation spectra of variable size argon clusters recorded in the Ar $2p$ regime at different average cluster size $\langle N \rangle$ [(d)–(h)]. The vertical dashed lines mark the energy positions of the distinct onsets in the fluorescence excitation spectra (see text for further details).

3 Results and discussion

Figure 1 shows a comparison of various energy scans in the Ar $2p$-excitation regime. The spectra have been recorded with the same energy resolution, so that the

band width of the primary photon source is identical, i.e. $E/\Delta E > 5\times10^3$ (see Sect. 2). The top spectra (a) and (b) show a comparison between the Ar^+ yield and the atomic fluorescence yield, respectively. The $2p^5n\ell$ Rydberg states are clearly resolved, so that the absolute energy scale and the energy resolving power are established by these spectra. A detailed discussion of these results has been published before [25] and is not subject of the present work.

Figure 1c shows the argon dimer cation ($Ar_2{}^+$) yield recorded at $\langle N\rangle = 200$ using the $\langle N\rangle$ calibration from reference [27]. This cation yield shows intense resonances in the near-edge regime, which are characteristically blue-shifted and broadened relative to the atomic transitions [35,36]. Mass lines of larger clusters are observed, these are known to yield similar spectral information as the dimer cation [36]. These small, singly charged fragments have been investigated before [37]. They are assigned to be the result of fission from doubly or multiply charged clusters, leading to a substantial kinetic energy release. We observe for the lowest energy features a dominant contribution of 4s-bulk excitons occurring at 245.15 eV and a weak signal from 4s-surface excitons at 244.65 eV. The corresponding transition occurs in the atom at 244.390 eV [38] (cf. Figs. 1a and 1b). The origin of these energy shifts has been discussed extensively before [35], so that Figure 1c essentially serves for a comparison with the series of fluorescence excitation spectra of variable size argon clusters and as an independent proof for the proper operation of the jet and the formation of clusters. Note that the photoion yields of mass-selected clusters and the fluorescence experiments were performed sequentially during the same beam time. Therefore, no conclusions regarding the fragmentation of charged clusters and fluorescence processes can be drawn. Fluorescence excitation spectra of variable size clusters are shown in Figures 1d–1h. The average cluster size $\langle N\rangle$ is systematically varied from $\langle N\rangle = 20$ (Fig. 1h) to $\langle N\rangle = 120$ (Fig. 1d). Note that the contribution of the atomic fluorescence has been subtracted from the raw spectra. Subsequently all spectra are normalized to the photon flux of the soft X-ray monochromator, so that only contributions from clusters remain. Evidently, the spectra suffer from low signal strength and thus a limited signal-to-noise ratio, since they were recorded with the same spectral resolution as the atomic spectra. This was necessary in order to prove whether discrete resonances from exciton states occur in fluorescence excitation spectra in the Ar 2p near-edge regime. Instead of smoothing the raw data, we have chosen to bin the data points together, by reducing the experimental point density by a factor of four, corresponding to an energy step width of 200 meV. This procedure improves significantly the signal-to-noise ratio without loosing spectral information for the dominant spectral features. This statement has been verified by applying the same procedure to the atomic spectra, for which all intense Rydberg features, that are narrower than the exciton features, are still observed. Note that the spectra shown in Figures 1d–1h are vertically scaled on the same pre-edge noise level, so that they can be compared to each other. This indicates that the fluorescence intensity increases substantially with $\langle N\rangle$. It is of negligible intensity in the low cluster regime, corresponding to $\langle N\rangle < 25$.

The experimental results on fluorescence yields of variable size clusters shown in Figures 1d–1h indicate that there are distinct differences compared to the spectra shown in Figures 1a–1c. The former spectra are comparable to our previous work [25], but the spectral resolution was insufficient at that time to draw any quantitative conclusions. Moreover, it was not attempted in that previous work to subtract the atomic contribution from the raw fluorescence yields. This is easily possible with the present data, since the atomic fluorescence occurs primarily upon excitation of Rydberg states, i.e. in a narrow spectral regime near the Ar 2p-edge from singly charged ions Ar^+ [32]. The atomic fluorescence vanishes in the Ar 2p continuum as a result of the dominant normal Auger effect in the Ar 2p continuum. The shape of the vanishing atomic fluorescence signal above ∼252 eV can be rationalized by post-collision interaction (cf. Fig. 1b) [39,40].

The cluster size dependence of the fluorescence excitation spectra indicates that there is hardly any signal detected at $\langle N\rangle = 20$, corresponding to a stagnation temperature of −25 °C at 5 bar stagnation pressure (see Fig. 1h). Note that at these conditions one observes strong contributions from clusters in photoionization mass spectra (cf. [36]). A weak fluorescence signal is observed at $\langle N\rangle = 25$ (cf. Fig. 1g, dashed lines) with two weak step-like onsets at photon energies of ∼248 eV and ∼250 eV (cf. Fig. 1g). At $\langle N\rangle = 40$ these are slightly red-shifted to 247.3 eV and 249.4 eV, respectively, and there is weak fluorescence intensity above the background level at photon energies above 246 eV (cf. Fig. 1f). Moreover, there is a broad resonance between 254 eV and 259 eV, which has been observed before [25,36]. The spectrum recorded at $\langle N\rangle = 60$ is similar in shape (see Fig. 1e). The clearest spectral dependence of the fluorescence is observed at $\langle N\rangle = 120$ (cf. Fig. 1d). The step-like onset energies are also observed at 247.3 eV and 249.4 eV and there is an onset above the background noise level at 246.6 eV.

These results indicate that there is almost no evidence for contributions to the fluorescence from variable size clusters from low-lying surface and bulk exciton states, which are superimposed to the step-like structures. These exciton features are clearly seen in the photoion yield spectra displayed in Figure 1c. Similarly, there is barely evidence in the fluorescence yield for the occurrence of the lowest 4s-exciton band around 245 eV [35,36]. The step-like onsets, which are observed in Figures 1d–1g, show a slight red-shift as a function of cluster size. We assign these step-like onsets to the Ar 2p ionization energies in clusters, which are known to shift to lower energy as a function of cluster size as a result of polarization screening [35,41]. Evidence for this assignment comes on one hand from the energy difference between both step-like features, which are separated by the spin-orbit splitting of 2.1 eV [42]. On the other hand, the energy position of the step-features is similar to the onset of direct 2p photoionization from bulk sites, as published by Björneholm et al. [35]. However,

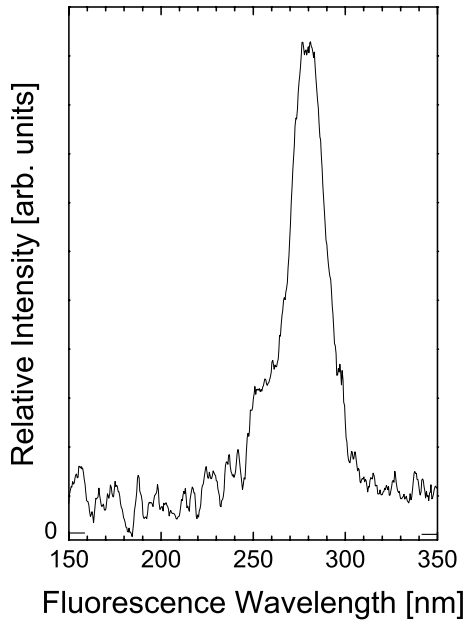

Fig. 2. Dispersed fluorescence spectrum recorded using undispersed, quasi-monochromatic undulator radiation at $E = 263$ eV. The sensitivity of the detector drops at wavelengths below 250 nm. Therefore, the signal shown in this regime is essentially due to background noise. Clusters are formed at a stagnation pressure of 5 bar and a stagnation temperature of -100 °C, corresponding to an average cluster size $\langle N \rangle = 80$.

a close inspection of the values derived from reference [35] indicates that the step-like onsets already occur at the low energy part of the features that are observed in photoelectron spectra, i.e. somewhat below the vertical core ionization energies of bulk sites. This is quite expected for a threshold signal, which extends into the regime below a vertical transition. In the case of small clusters the onsets of the fluorescence yield occur at somewhat higher energies, which are assigned to weak fluorescence from surface sites. The size evolution of the signal strength indicates that radiative relaxation comes preferably from bulk sites of large clusters. This interpretation is also in agreement with the occurrence of the broad continuum feature between 254 eV and 259 eV, which is found in total electron yields of large clusters [36]. It is a result of single and multiple scattering processes of bulk sites. Furthermore, the weak fluorescence intensity that is observed at even lower energy than the $2p$-ionization energies of bulk sites may be due to high-lying exciton states of bulk sites.

The wavelength regime of fluorescence radiation that contributes to the excitation spectra is shown in Figure 2. It consists of a broad resonance located in the wavelength regime between 250 nm and 300 nm. Such a feature has already been observed in our previous work [25], which was performed under low resolution conditions compared to the present set-up. The spectrum shown in Figure 2 indicates that there are indeed no discrete features including atomic lines in the spectral regime under investigation. But there is a remarkable difference in comparison with the previous work, where a broad double-hump feature was observed with maxima at 200 nm and 270 nm, respectively [25]. The short wavelength feature near 200 nm is not observed in the present work. A plausible explanation for this difference is found by the fact that different experimental set-ups are used. The previous one was optimized for the spectral regime around 200 nm [25], whereas the present one looses substantially detection sensitivity with decreasing wavelength [30]. Thus, we expect that the transmission drops significantly below 250 nm and only the long wavelength feature is detected by the present set-up (cf. Sect. 2). The results on fluorescence excitation spectra indicate, however, that the observed energy dependence of the fluorescence yield is comparable to previous work [25].

A comparison with other studies on "third continuum" fluorescence of gaseous and solid argon indicates that the present experimental conditions give rise to the emission of somewhat longer wavelength UV-radiation, than that observed in previous studies on gaseous and solid argon [10–22]. This gives evidence for the fact that likely somewhat different processes are probed in the present work. Especially, in solid argon one observes a broad photon- or electron-induced luminescence band around 200 nm, where the fluorescence extends only up to 225 nm [12,20]. Previous work by Ogurtsov et al. [21] indicates that the fluorescence near 200 nm is clearly due to singly charged argon, which follows from the low excitation energies in the outer shell excitation regime, where double ionization cannot occur. This result is in agreement with work of Amirov et al. [22], who developed a model in order to rationalize the emission of continua of UV-radiation. Specifically, it was proposed that the continua can be attributed to transitions from low-lying Rydberg states of singly charged dimer cations to low repulsive states. Note that results published by Krötz et al. [18] and Wieser et al. [19] give different assignments of the radiating species near 200 nm by considering doubly charged dimers and trimers. Furthermore, results from high-pressure gases that are ionized by discharges in high pressure plasmas [16], pulsed X-rays [17], heavy ion impact [18,19], and α-particles [10,13] yield fluorescence emission up to wavelengths of 300 nm, which is in the same regime as in the present work.

The fluorescence observed in the present work indicates that this process occurs almost exclusively in the $2p$-continuum. The fact that there is hardly any evidence for UV-fluorescence from clusters in the pre-edge regime already indicates that the process is initiated by the occurrence of the $2p$-core hole and the ejection of the core electron into the $2p$-continuum. It is clear that this process is tightly related to double or even multiple ionization of clustered atoms, that are preferably located in the bulk of the clusters. Further support for this interpretation comes from the step-like onset behavior of the fluorescence excitation spectra, since resonant excitations into low-lying near-edge exciton states lead preferably via spectator autoionization to singly charged products. It is, however, not clear that necessarily doubly charged atoms are the origin of the fluorescence photons in clusters.

Time resolved experiments indicate that the radiative processes, especially those leading to fluorescence at wavelengths larger than 240 nm, occur in the nanosecond time regime [19]. Such temporal evolution is slow compared to the regime of de-excitation processes, which occur after the formation of the 2p-core hole. Electronic relaxation of the core hole via the Auger decay takes place in the femtosecond time regime, as it is known from results in the frequency and time domain on argon or other rare gases [43,44]. The key point of the de-excitation processes is the fate of the initially doubly or triply charged atom that is produced after absorption of an X-ray photon, if it is bound in a cluster, especially in its bulk interior. Our previous assignment [25] was in line with the model of Langhoff [14,15], who considered the formation of charge transfer excimers. More recent theoretical work by Cederbaum and co-workers predicts that there are efficient, ultrafast energy transfer processes active in inner-valence shell-excited clusters, which take place in the femtosecond time regime [1–5]. These are termed interatomic Coulombic decay (ICD). The lifetime of these multiply charged states is significantly reduced for bulk sites compared to dimers. Related work predicts that ICD is not only present in inner-valence-excited, but also in core-excited clusters [6]. This implies that ICD will follow the Auger decay, which is localized to the excited atom. The ICD lifetime is expected to drop with the number of nearest neighbors of the excited center [4,6], implying that bulk sites are most sensitive to this ultrafast process. Experimental evidence for the occurrence of ICD has been found recently, which also includes short lifetimes of the order of a few femtoseconds [7–9].

It is clear that de-excitation of 2p-excited argon clusters is dominated by the LMM-Auger decay, yielding an excited dication [45]. Previous work by Santra and Cederbaum on core-excited neon dimers as a simple model system indicates that more than 20% of all dications that are produced by the Auger process will undergo ICD forming a trication [6]. The doubly charged species are calculated to be inner-valence shell excited. Considering the reduced ICD lifetime of bulk sites mentioned above [4,6], the importance of ICD will increase with cluster size. A result of ICD is, that sites next to the core-excited atom undergoing the Auger decay become singly charged, where the net charge of the cluster becomes at least +2. The charges located on different atoms, as a result of the ICD-mechanism, will repel each other. This may even lead to fission [46], if doubly charged clusters contain less than 91 atoms [47] or triply charged ones less than 226 atoms [48].

Additionally, one may consider that the Auger electron can also be inelastically scattered at neighboring sites within the cluster (cf. [49]), a process also occurring in the femtosecond time regime. This process will also lead to triple or multiple ionization of clusters, similar to ICD. Such electron impact ionization of the nearest neighbor shell within a cluster or a solid will preferably occur in large clusters and solids, where inelastic scattering is most efficient for sites deep in the bulk. This is unlike ICD, which is mostly sensitive to the nearest neighbor shell [4,6]. Thus, in ICD the shells of further distant sites are less important than in inelastic scattering. As a result, ICD is likely more important, probably even dominating for bulk sites of small clusters, i.e. the cluster size regime under investigation.

De-excitation processes of resonantly core-excited atoms and molecules lead to the formation of excited cations. In these systems the resonant Auger effect is most efficient for the formation of the excited, singly charged species, which are stabilized by the emission of fluorescence radiation in the ultraviolet/visible regime [32,33]. In the case of weakly bound clusters, there is the additional ICD process following the Auger decay, leading to charge de-localization via an energy transfer. As a result, singly charged, excited moieties in clusters are formed, which cannot be stabilized via the emission of electrons. Their radiative de-excitation is assumed to be observed in the present experiments. Moreover, the Auger decay may also lead to the formation of excited dications, which are expected to emit radiation, but likely in a different wavelength regime. The central question is in which wavelength regime singly or doubly charged moieties within a cluster decay via the emission of ultraviolet radiation. Considering the work by Wieser et al. [19], the emission of fluorescence radiation near 200 nm, which was observed in our previous work [25], is a result of sites that contain doubly charged moieties. In contrast, long wavelength radiation, observed in the present experiments around 280 nm is most likely due to the emission from excited, singly charged sites. These sites are assigned to be preferably formed via ICD in the cluster size regime under investigation using the present experimental results. This result provides evidence that fluorescence spectroscopy is a sensitive probe for the predicted ICD-mechanism of core-excited clusters. Finally, we note that this result goes beyond recent experimental work, where photoelectron spectroscopy has been used as a probe for the occurrence of ICD in the inner valence shell regime [7–9].

4 Conclusions

We have investigated the ultraviolet fluorescence of variable size argon clusters in the Ar 2p-excitation regime. The present results are obtained with substantially improved resolution of the primary soft X-ray monochromator, indicating that excitation of low-lying exciton states in the near-edge regime gives no significant contribution to the fluorescence yield. High resolution dispersed fluorescence experiments indicate that only a broad molecular band occurs in the regime $\lambda < 300$ nm, similar to previous work and related experiments on gaseous and condensed argon [10–22]. The present assignment of the processes occurring in 2p-excited clusters leads to the conclusion that core level excitation initiates the formation of excited, molecular moieties within a cluster. Rapid electronic relaxation via the Auger decay and subsequent energy transfer processes (ICD) lead primarily to the formation of singly and doubly charged, excited moieties within

clusters, where the former ones are assigned to be the origin of the detected fluorescence in the ultraviolet regime near 280 nm.

Financial support by the Deutsche Forschungsgemeinschaft, the Franco-German PROCOPE program (DAAD, Germany), the European Community – Research Infrastructure Action under the FP6 "Structuring European Research Area" Program (contract R II 3-CT-2004-506008), and the Fonds der Chemischen Industrie is gratefully acknowledged.

References

1. L.S. Cederbaum, J. Zobeley, F. Tarantelli, Phys. Rev. Lett. **79**, 4778 (1997)
2. J. Zobeley, L.S. Cederbaum, F. Tarantelli, J. Phys. Chem. A **103**, 11145 (1999)
3. R. Santra, J. Zobeley, L.S. Cederbaum, N. Moiseyev, Phys. Rev. Lett. **85**, 4490 (2000)
4. R. Santra, J. Zobeley, L.S. Cederbaum, Phys. Rev. B **64**, 245104 (2001)
5. R. Santra, L.S. Cederbaum, Phys. Rep. **368**, 1 (2002)
6. R. Santra, L.S. Cederbaum, Phys. Rev. Lett. **90**, 153401 (2003)
7. S. Marburger, O. Kugeler, U. Hergenhahn, T. Möller, Phys. Rev. Lett. **90**, 203401 (2003)
8. T. Jahnke, A. Czasch, M.S. Schöffler, S. Schössler, A. Knapp, M. Käsz, J. Titze, C. Wimmer, K. Kreidi, R.E. Grisenti, A. Staudte, O. Jagutzki, U. Hergenhahn, H. Schmidt-Böcking, R. Dörner, Phys. Rev. Lett. **93**, 163401 (2004)
9. G. Öhrwall, M. Tchaplyguine, M. Lundwall, R. Feifel, H. Bergersen, T. Rander, A. Lindblad, J. Schulz, S. Peredkov, S. Barth, S. Marburger, U. Hergenhahn, S. Svensson, O. Björneholm, Phys. Rev. Lett. **93**, 173401 (2004)
10. T.D. Strickler, E.T. Arakawa, J. Chem. Phys. **41**, 1783 (1964)
11. J. Jortner, L. Meyer, S.A. Rice, E.G. Wilson, J. Chem. Phys. **42**, 4250 (1965)
12. E.E. Huber Jr, D.A. Emmons, R.M. Lerner, Opt. Commun. **11**, 155 (1974)
13. G. Klein, M.J. Carvalho, J. Phys. B **14**, 1283 (1981)
14. H. Langhoff, Opt. Commun. **68**, 31 (1988)
15. H. Langhoff, J. Phys. B **27**, L709 (1994)
16. C. Cachoncinlle, J.M. Pouvesle, F. Davanloo, J.J. Coogan, C.B. Collins, Opt. Commun. **79**, 41 (1990)
17. E. Robert, A. Khacef, C. Cachoncinlle, J.M. Pouvesle, Opt. Commun. **117**, 179 (1995)
18. W. Krötz, A. Ulrich, B. Busch, G. Ribitzki, J. Wieser, Phys. Rev. A **43**, 6089 (1991)
19. J. Wieser, A. Ulrich, A. Fedenev, M. Salvermoser, Opt. Commun. **173**, 233 (2000)
20. A.M. Boichenko, V.I. Derzhiev, A.G. Zhidkov, A.A. Kuznetsov, S.S. Sulakshin, V.F. Tarasenko, S.I. Yakovlenko, Opt. Spektrosk. **68**, 5 (1990)
21. A.N. Ogurtsov, E.V. Savchenko, J. Becker, M. Runne, G. Zimmerer, J. Luminesc. **76-77**, 478 (1998)
22. A.Kh. Amirov, O.V. Korshunov, V.F. Chinnov, J. Phys. B **27**, 1753 (1994)
23. C. Cachoncinlle, J.M. Pouvesle, G. Durand, F. Spiegelmann, J. Chem. Phys. **96**, 6085 (1992); G. Caconcinlle, J.M. Pouvesle, G. Durand, F. Spiegelmann, J. Chem. Phys. **96**, 6093 (1992)
24. A.V. Zaitsevskii, A.I. Demet'ev, Opt. Commun. **86**, 461 (1991)
25. E. Rühl, C. Heinzel, H.-W. Jochims, Chem. Phys. Lett. **211**, 403 (1993)
26. S. Bernstorff, W. Braun, M. Mast, W. Peatman, T. Schroeter, Rev. Sci. Instrum. **60**, 2097 (1989)
27. R. Karnbach, M. Joppien, J. Stapelfeldt, J. Wörmer, T. Möller, Rev. Sci. Instrum. **64**, 2838 (1993)
28. J. Farges, M.F. de Feraudy, B. Raoult, G. Torchet, J. Chem. Phys. **84**, 3491 (1986)
29. A. Marquette, Ph.D. thesis, Université de Lille I, Lille (2000)
30. A. Marquette, M. Gisselbrecht, W. Benten, M. Meyer, Phys. Rev. A **62**, 22513 (2000)
31. L. Minnhagen, Ark. Fys. **25**, 203 (1964)
32. R. Flesch, H.-W. Jochims, J. Plenge, E. Rühl, Phys. Rev. A **61**, 62504 (2000)
33. A. Marquette, M. Meyer, F. Sirotti, R.F. Fink, J. Phys. B **32**, L325 (1999)
34. D.L. Judge, G.L. Weissler, J. Chem. Phys. **48**, 4590 (1968)
35. O. Björneholm, F. Federmann, F. Fössing, T. Möller, Phys. Rev. Lett. **74**, 3017 (1995)
36. E. Rühl, C. Heinzel, A.P. Hitchcock, H. Baumgärtel, J. Chem. Phys. **98**, 2653 (1993)
37. E. Rühl, C. Schmale, H.W. Jochims, E. Biller, M. Simon, H. Baumgärtel, J. Chem. Phys. **95**, 6544 (1991)
38. G.C. King, M. Tronc, F.H. Read, R.C. Bradford, J. Phys. B **10**, 2479 (1977)
39. A. Niehaus, J. Phys. B **10**, 1845 (1977); P. van der Straten, R. Morgenstern, A. Niehaus, Z. Phys. D **8**, 35 (1988)
40. W. Eberhardt, S. Bernstorff, H.W. Jochims, S.B. Whitfield, B. Crasemann, Phys. Rev. A **38**, 3808 (1988)
41. O. Björneholm, F. Federmann, F. Fössing, T. Möller, P. Stampfli, J. Chem. Phys. **104**, 1846 (1996)
42. A. Knop, H.W. Jochims, A.L.D. Kilcoyne, A.P. Hitchcock, E. Rühl, Chem. Phys. Lett. **223**, 553 (1994)
43. J. Stöhr, *NEXAFS Spectroscopy* (Springer, Berlin, 1992)
44. M. Drescher, M. Hentschel, R. Kienberger, M. Uiberacker, V. Yakovlev, A. Scrinzi, T. Westerwalbesloh, U. Kleineberg, U. Heinzmann, F. Krausz, Nature **419**, 803 (2002)
45. E.J. McGuire, Phys. Rev. A **11**, 1880 (1975)
46. E. Rühl, C. Heinzel, H. Baumgärtel, M. Lavollée, P. Morin, Z. Phys. D **31**, 245 (1994)
47. P. Scheier, T.D. Märk, J. Chem. Phys. **86**, 3056 (1987)
48. P. Scheier, T.D. Märk, Chem. Phys. Lett. **136**, 423 (1987)
49. R. Scheuerer, P. Feulner, G. Rocker, L. Zhu, D. Menzel, *DIET IV* (Springer, Berlin, 1990), p. 235